Free-surface flow in horizontally rotating cylinder: experiment and simulation

You may also be interested in:

Free-surface flow in horizontally rotating cylinder: experiment and simulation

J Bohacek[1]**, A Kharicha**[2, 4]**, A Ludwig**[1]**, M Wu**[2]**, A Paar**[3]**, M Brandner**[3]**, L Elizondo**[3] **and T Trickl**[3]

[1]Dept. of Metallurgy, Montanuniversitaet Leoben, Austria
[2]Christian Doppler Lab for Advanced Simulation of Solidification and Melting, Montanuniversitaet Leoben, Austria
[3]Eisenwerk Sulzau-Werfen, R. & E. Weinberger AG, Austria

E-mail: abdellah.kharicha@unileoben.ac.at

Abstract. The horizontal centrifugal casting process targets on a liquid layer with a uniform thickness. To achieve this, the rotations of the mold have to be large enough so that the liquid can pick up the speed of the mold. In the present paper, an experiment was conducted using a laboratory plexi-glass mold with water as a working fluid. Starting with an initial volume fraction of liquid resting in the bottom of the mold, the mold rotations were gradually increased from 0 rpm to max rpm and a new position of the contact line was recorded. In addition, first critical rpm was recorded, at which the transition from the liquid pool to a uniform liquid layer occurred. While gradually going back from max rpm to 0 rpm, second critical rpm was recorded, at which the uniform liquid layer collapsed. The experiment was compared with the numerical simulation solving the modified shallow water equations using the Newton-Raphson method with the Wallington filter.

1. Introduction

The horizontal centrifugal casting (HCC) is a process at which it is among other things necessary to use high enough rotations of the cylindrical mold, so that the liquid picks up the speed of the rotating mold and creates a layer of a uniform thickness around the mold circumference. In fact, also upper limit exists such that too high rotations can lead to excessive vibrations of the system, which are commonly related to undesired hoop stresses in the product [1]. An experimental and numerical study of the first is a main target of the present paper. The experiment and the numerical simulation are discussed in detail in section 2 and section 3, respectively.

The survey of related experimental articles showed that most researchers concentrated on free-surface patterns corresponding to mold rotations at which the liquid was already moving with the speed of the mold. For example in [2], Martinez identified several different wave patterns on the free surface of the liquid layer and also stated that some of the wave patterns are related to mold vibrations and deformations. In [3], the effort of Esaka moved from observing free surface patterns to investigation of what is happening inside the transparent solidifying liquid. By attaching a high-speed camera to the rotating mold, a relative movement of a selected equiaxed crystal could be analysed. During each rotation of the mold the position of the equiaxed crystal oscillates due to the pumping effect caused by the gravity. Moreover, the selected equiaxed crystal slowly moves in the anti-

---

[4] To whom any correspondence should be addressed.

rotational direction due to a certain slip between the liquid bulk and the mold. The pumping effect as a result of interaction between the inertia force and the gravity is also responsible for having a thicker layer in the top than in the bottom. In another experimental study [4], Prasad searched for minimal mold rotations required to form a uniform liquid layer. Liquids with higher viscosities and lower volume fractions naturally require lower rpm. He also pointed out that minimal rpm is influenced by the formation of the Ekman vortex near the mold extremities. The liquid in a longer mold will pick up the speed easier than in a shorter mold of the same diameter. Other investigators (e.g. [5]) were more focused on examination of coating flows inside a horizontally rotating cylinder generally containing a small amount of a very viscous liquid. A rich variety of flow patterns has been observed.

Unlike flows in the horizontal centrifugal casting, the coating flows were intensively investigated using the thin-film lubrication equations often in dimensionless form. For example in [6], Hosoi used the lubrication theory to capture so-called shark-teeth pattern, pseudo-stationary pendants, and periodic sloshing. Numerical tools used in the modelling of the horizontal centrifugal casting generally rely on commercial CFD packages namely the VOF free-surface tracking [7]–[9]. In our previous work we applied so-called shallow water equations especially for the purpose of major computational time savings [10]. In the present paper, in addition to the experiment discussed later we introduced modified shallow water equations in dimensionless form solved by the iterative Newton-Raphson method [11]. The objective of the present numerical study is to demonstrate the capability of capturing the main flow features. The numerical model is compared with the experiment.

2. Experimental set-up

Here, the experiment focuses on analysis of fluid flow in the horizontal centrifugal casting process namely on estimation of the contact line position within a given range of Froude numbers. The dimensionless Froude number Fr is defined as ratio between the centrifugal inertia and the gravity $\left(\Omega\sqrt{R/g}\right)$, where Ω is the angular frequency of the mold in rad/s, R is the inner mold radius, and g is the gravitational acceleration. The definition of the contact line is pictured in figure 1. In addition, we looked for a critical Froude number $\uparrow Fr_c$ at which transition from the liquid pool to a uniform layer occurred. We also looked for other critical Froude number $\downarrow Fr_c$ at which raining [12] appeared and the originally uniform layer collapsed. For this experiment, a laboratory plexi-glass mold was used with the length of 705 mm and the inner diameter of 285 mm. On one side, the mold is connected through a shaft to an AC motor, whose speed can be varied via a frequency changer from 0 rpm to 500 rpm. On the other side, the mold is opened so that the mold filling can be easily done. The schematic of the whole device is illustratively shown in figure 2. Snapshots of the free surface were taken by the digital camera CASIO EX-F1 (F2.7, 1/1000) mounted approximately coaxially with the mold axis, placed in a laboratory (non-rotating) reference frame. The amount of 1 liter of water at room temperature was used as a working liquid. The experiment involved the following steps:

- Pour a specific amount of liquid.
- For the post-processing namely automatic axis insertion, take a picture of the calm free surface.
- Very slowly increase mold rotations and at defined rpm take a picture of the actual free surface.
- During increasing mold rotations check for $\uparrow Fr_c$.
- After exceeding $\uparrow Fr_c$ very slowly decrease mold rotations and check for $\downarrow Fr_c$.

The experiment was followed by a simple image post-processing. The snapshot with the calm free surface was used to transform cylindrical coordinate system in perspective projection and insert tangential ticks (figure 3) eventually copied into all other pictures. From each picture, the contact line position was extracted and plotted against the corresponding Froude number Fr (figure 5). On horizontal axis we also marked the location of both, $\uparrow Fr_c$ and $\downarrow Fr_c$. Note that $\uparrow Fr_c$ required to form a uniform layer is generally much higher than $\downarrow Fr_c$ corresponding to the moment when the uniform layer collapses. The magnitude of $\downarrow Fr_c$ is approaching unity ($\downarrow Fr_c \rightarrow 1$) indicating an exact balance between the centrifugal force and the gravity. The theoretical $\downarrow Fr_c$ ($\downarrow Fr_c = 1$) is shown as a dot-and-dashed line on horizontal axis in figure 5.
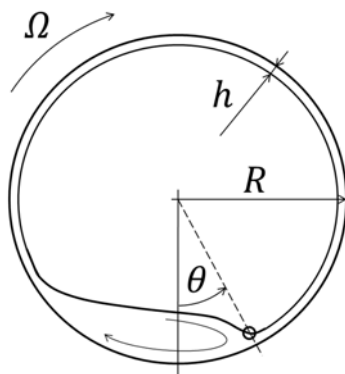
Figure 1. Schematic diagram of a cross section of the rotating plexiglass mold. Angle θ signifies tangential position. (The actual magnitude of angle θ corresponds to the contact line position.
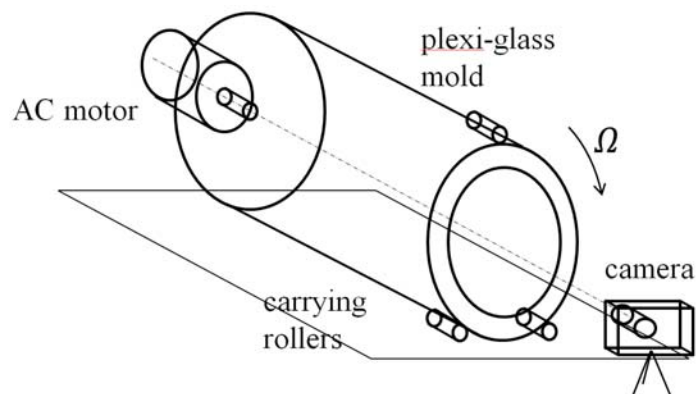

Figure 2. Sketch of the experimental set-up.

In the reality, $\downarrow Fr_c$ is always greater than unity due to the fact that Fr is defined using the mold radius R and not the radius measured from the free surface to the mold center. Next, it is also the relative velocity field generated by the pumping effect and inherent vibrations that increase $\downarrow Fr_c$. A different story applies to $\uparrow Fr_c$ where it is the ratio between the viscous forces and the gravity $\left(\alpha = \sqrt{v\Omega R/gh^2}\right)$ responsible for picking up the liquid, where h and v are the thickness of the liquid film and the kinematic viscosity. $\uparrow Fr_c$ can be estimated from setting $\alpha = 1$ and substituting Fr into α. Having the Reynolds number defined as $Re = \Omega h^2/v$, $\uparrow Fr_c$ becomes simply $\sqrt{Re}$. –However, when the turbulence is present the effective viscosity should be used instead. Hence, calculation of $\uparrow Fr_c$ is not trivial. In addition to Fr analysis, in figure 4 one can notice so-called shark-teeth pattern studied earlier in [14]. The range of occurrence is also demarcated in the figure 5. In the next section we attempt to simulate the aforementioned scenario using modified shallow water equations with more details given for example in [15]–[17].
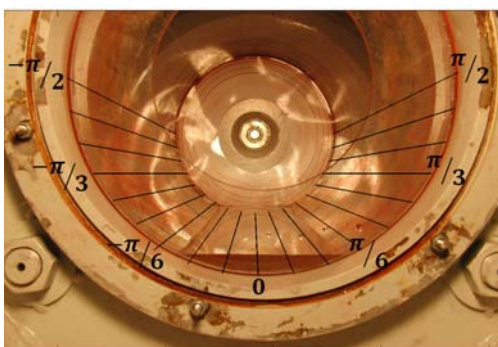

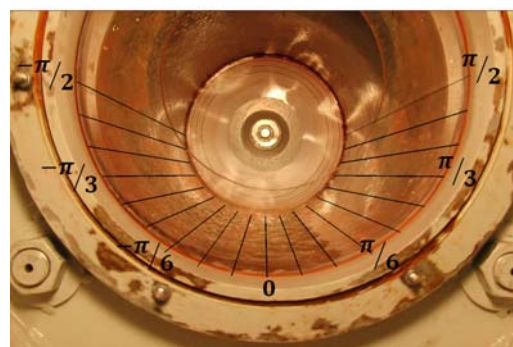**Figure 3.** Snapshot of the calm free surface. The liquid volume fraction of 1 liter.

Figure 4. Shark-teeth pattern at $Fr \cong 1.3$ (105 rpm).

3. Numerical model

Here, the objective of the numerical model is to examine whether the modified shallow water equations (SWE) can capture the main flow features such as the recirculation region in the bottom of the mold, correct position of the contact line, $\uparrow Fr_c$ and $\downarrow Fr_c$. The SWE belong to the group of hydrostatic models [18]. For the cylindrical geometry, the original SWE were modified and can be written as the following:

$$h_t + (hu)_x = 0 \tag{1}$$

$$(hu)_t + \left(hu^2 + \frac{1}{2} gh^2 \cos\theta + \frac{1}{2R}(hu)^2 \right)_x = -gh\sin\theta - 3v\frac{u - \Omega R}{h} \tag{2}$$
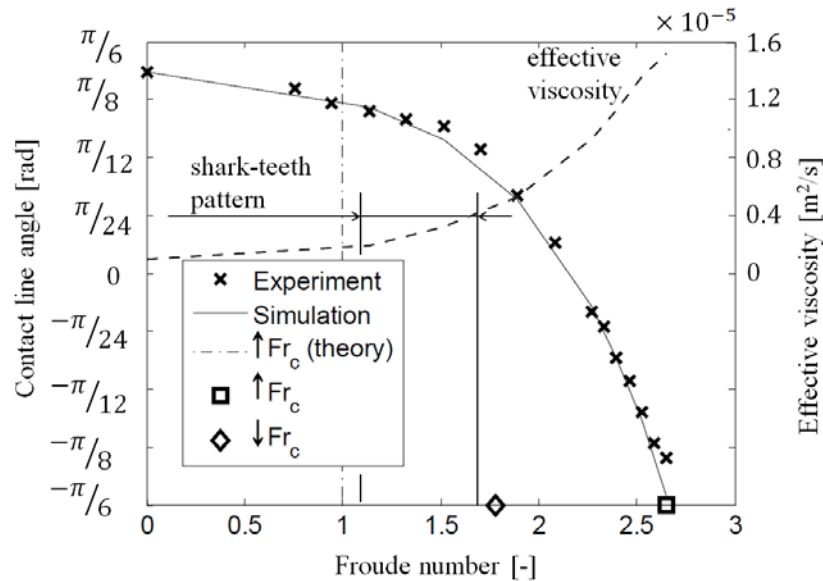

Figure 5. Contact line vs. Froude number for the liquid volume fraction of 1 liter obtained from the experiment and the simulation. The occurrence range of shark-teeth pattern is demarcated. $\uparrow Fr_c$ and $\downarrow Fr_c$ are marked on the horizontal axis. Effective viscosity used in simulation is shown in dashed line.

In the present study, the axial momentum was omitted from the calculation. Equations (1)–(2) are the continuity equation and the momentum equation for the tangential direction. Subscripts t and x denote temporal and spatial derivatives, respectively. Since $h \ll R$, the Cartesian coordinate system is used and the tangential coordinate x is defined as $x = R\theta$ with $\theta = 0$ rad in the bottom of the mold. In (2), the second and the third term in the fluxes $(...)_x$ represent the gradient of the hydrostatic pressure integrated over the liquid height h, resulting from the radial component of the gravity and the motion in a curved geometry, respectively. On the rhs, the first term corresponds to the tangential component of the gravity, while the last term denotes the bed shear stress with the moving mold wall assuming a parabolic velocity profile [19]. Then, equations (1)–(2) were further rewritten in the dimensionless form. Dimensionless variables in the problem become

$$\tilde{h} = \frac{1}{R}h \qquad \tilde{u} = \frac{1}{\Omega R}u \qquad \tilde{t} = \frac{1}{\Omega}t$$

$$Fr = \Omega \left(\frac{R}{g}\right)^{1/2} \qquad Re = \frac{\Omega R^2}{v} \tag{3}$$

Equations (1)–(2) in the dimensionless form become (Note that the tilde ~ was dropped)

$$h_t + (hu)_x = 0 \tag{4}$$

$$(hu)_t + \left(hu^2 + \frac{1}{2} Fr^{-2} h^2 \cos \theta + \frac{1}{2} (hu)^2 \right)_x = -Fr^{-2} h \sin \theta - 3 Re^{-1} \frac{u - 1}{h} \tag{5}$$

Equation (4)–(5) can be categorized as the non-linear conditionally hyperbolic equations. The hyperbolicity can be lost exclusively due to the negative second term in the fluxes $(...)_x$ of (5) in the upper part of the mold. To solve (4)–(5) an implicit scheme for the time differencing was used with a timestep Δt chosen by step doubling. The resulting equations were solved simultaneously via the Newton-Raphson method using <5 iterations. Handling of dry cells was remedied by adding an artificial viscosity term Dh_{xx} to (4) with the diffusivity term D, acting only when $h \to 0$. In addition, dispersive errors were damped via the Wallington filter [20]. In figure 6, free surface patterns are shown at different Froude numbers Fr. The corresponding position of the contact line is plotted along with the experimental data in figure 5. As already mentioned, the kinematic viscosity needs to be replaced with the effective viscosity due to turbulent effects. Since the turbulent effects are not accounted for by (4)–(5), the effective turbulent viscosity is obtained by solving the inverse task with the objective function equal to the difference between the computed and measured position of the contact line. The calculated effective viscosity is shown on the second y-axis in figure 5. The higher rotations of the mold will produce a more turbulent flow with a higher effective turbulent viscosity.
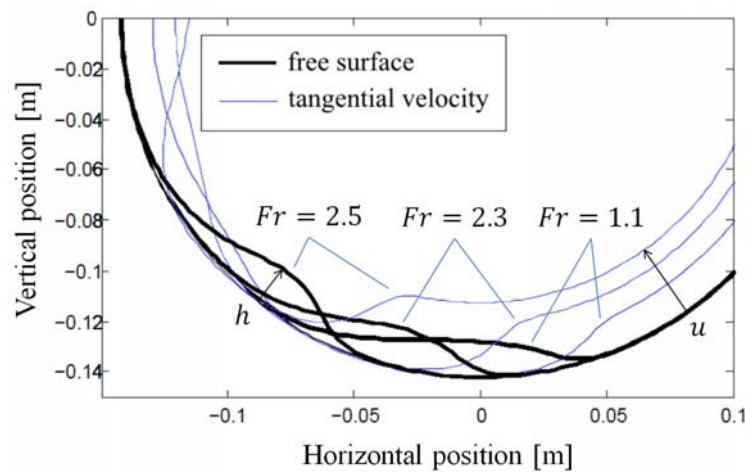

Figure 6. Calculated free-surface and magnitudes of average tangential velocity shown at different Froude numbers Fr.

In figure 7, we show a detail of the recirculation zone at $Fr = 2.3$. Note that although the 2D velocity vector field is not directly calculated from (4)–(5), it can be reconstructed with the help of the continuity equation, 1D field of tangential velocities u, and the assumption of a parabolic velocity profile.
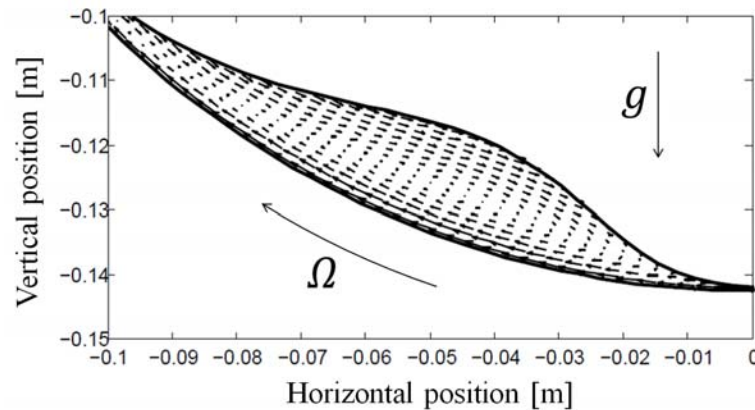
Figure 7. Recirculation zone with a reconstructed velocity vector field at $Fr = 2.3$.

4. Conclusions

Using a laboratory plexi-glass mold we performed experiments with water at room temperature as a working fluid. Here, only a single liquid volume fraction was tested (1 liter). During the experiment the rotations were gradually increased and the position of the contact line was recorded. In addition, $\uparrow Fr_c$ required for the liquid to pick up the speed of the mold and $\downarrow Fr_c$ necessary to prevent raining and consequent collapse of the uniform liquid layer were examined. The experiment showed that $\uparrow Fr_c$ is generally much higher than $\downarrow Fr_c$. While it is possible to estimate $\downarrow Fr_c$ quite reliably using the condition of the hydrostatic balance, it is hard to draw any quantitative judgement on $\uparrow Fr_c$ due to due to strong turbulent effects adjusting the effective viscosity. During the industrial centrifugal casting process namely during the pouring stage, it is necessary to keep $Fr \geq \uparrow Fr_c$ in order to pick up the speed of the mold. On the other hand, once the pouring is finished and the liquid forms a uniform layer, it is apparently sufficient to keep Fr slightly larger than 1 ($\downarrow Fr_c$). The positive difference is needed to compensate the pumping effect and mold vibrations.

In addition to the experiment, we investigated whether the modified shallow water equations are able to capture the recirculation region formed close to the bottom of the mold. We concluded that the mathematical model possess this ability, however; requires an estimation of the effective viscosity. In fact, this relatively simple mathematical model can also successfully predict the pumping effect caused by the gravity. This topic is not covered in the present study. For the future, we plan to test wide variety of liquid volume fractions and liquids with different viscosities.

5. Acknowledgement

6. References

[1]   Mandal D 2008 Special Metal Casting and Forming (CAFP) pp 1-19

[2]   Martinez G, Garnier M and Durand F 1987 *Appl. Sci. Res.* **44** pp 225–239

[3]   Esaka H, Kawai K, Kaneko H and Shinozuka K 2012 *Mater. Sci. Eng.* **33** 012041

[4]   Keerthiprasad K S, Murali M S, Mukunda P G and Majumdar S 2010, *Front. Mater. Sci. China* **4** pp 103–110

[5]   Thoroddsen S T, Mahadevan L 1997 *Exp. Fluids* **23** pp 1–13

[6]   Hosoi A E, Mahadevan L 1999 *Phys. Fluids* **11** pp 97–106

[7]   Xu Z, Song N, Tol R V, Luan Y and Li D 2012 *Mater. Sci. Eng.* **33** 012030

[8]   Keerthiprasad K S, Murali M S, Mukunda P G and Majumdar S 2010 *Metall. Mater. Trans.* B **42** pp 144–155

[9]   Kaschnitz E 2012 *Mater. Sci. Eng.* **33** 012031

[10]   Bohacek J, Kharicha A, Ludwig A and Wu M 2014 *ISIJ Int.* **54**(2) pp 266–274

[11]   Tjalling J Y 1995 *SIAM Rev.* **37**(4) pp 531–551

[12]   Lebeau T C 2008 *MSc thesis* University of Alabama p 16

[13]   Bagheri J, Das S K 2013 J. Appl. Computat. Math.

[14]   Krasnopol'skaya T S, van Heijst G J F, Voskamp J H and Trigger S A 2001 *Int. Appl. Mech.* **37**(7) pp 929–934

[15]   Bohacek J, Kharicha A, Ludwig A and Wu M 2013 *Mater. Sci. Eng.* **33** 012032

[16]   Bohacek J, Kharicha A, Ludwig A and Wu M 2015 *Appl. Math. Comput.* **267** pp 179–194

[17]   Kharicha A, Bohacek J, Ludwig A and Wu M 2015 *J. Fluids Eng.* **137**(11) 111105

[18]   George D. L. 2006 *PhD thesis* University of Washington, p 36

[19]   Murillo J, Gracía-Navarro P 2012 *J. Comput. Phys.* **231**, pp 1963–2001

[20]   Wallington C E 1962 *J. Roy. Meteor. Soc.* **88** pp 437–484